

# Optimum channel intrusion depth for uniform flow distribution at header-channel junctions<sup>†</sup>

Jun Kyoung Lee\*

School of Mechanical Engineering and Automation, Kyungnam University, Masan, 631-701, Korea

(Manuscript Received August 11, 2009; Revised February 23, 2010; Accepted April 15, 2010)

## Abstract

The ultimate goal of this work is to find the optimal condition for the even distribution of two-phase mixture at header-channel junctions simulating the corresponding parts of compact heat exchangers. The cross section of the header and the channels were 14 mm × 14 mm and 12 mm × 1.6 mm, respectively. Two different distances between channels (10 and 21.6 mm) and four different intrusion depths (0, 1.75, 3.5 and 7 mm) beyond the inner wall of the header were tested for the mass flux and the mass quality ranges of 70 - 165 kg/m<sup>2</sup>s and 0.3 – 0.7, respectively. Air and water were used as the test fluids. The flow distribution pattern was relatively insensitive to the channel distance because the flow configuration inside the header remained almost unchanged. On the other hand, the distribution pattern was changed drastically with the intrusion depth of the channels. The optimum intrusion depth for even flow distribution was identified to be 1/8 of the hydraulic diameter of the header cross-section for the experimental conditions tested in the present work.

**Keywords:** Flow distribution; Header-channel junctions; Distance between channels; Intrusion depth; Uniform flow distribution

## 1. Introduction

Problem of flow mal-distribution inside the heat exchanging system has been becoming of interest since the state of flow distribution determines the heat transfer performance seriously. Especially, flow distribution from a partitioned header to parallel channels as shown in Fig. 1 is very important because non-uniform distribution makes the thermal performance deteriorated, significantly. According to Kulkarni et al. [1], the performance reduction in micro-channel evaporators by flow mal-distribution could be as large as 20%.

In many cases, due to the flow mal-distribution, the flow rates in the channels are not the same (Lee [2], Lee and Lee [3], Hrnjak [4] and etc.). For the case of two-phase flow, the situation becomes even worse. Lack of liquid flow in some channels results in surface dryout and poor heat transfer. In case of air-cooling system, this makes the air temperature non-uniform; if the local temperature becomes higher than the dew point temperature, the dehumidification effect is deteriorated; on the other hand, if the local temperature is below the freezing point, an uneven frosting of the evaporator may occur. (Fei et al. [5]) Besides, the flooded refrigerant tubes may bring out the problem of control stability of the thermal expansion valve.

(Zietlow et al. [6])

Lee [2] have performed experimental works for a header (14 mm × 14 mm) with fifteen parallel channels (12 mm × 1.6 mm) with an end plate. The distribution pattern of the flow through the channels was determined by the flow recirculation near the end plate. The header flow consists of three zones, denoted by regions A, B and C, as illustrated in Fig. 2. At the entrance portion (region A) and at the immediate upstream of the end plate (region C), less amount of liquid flow was separated out through the channels as the two-phase mixture proceeds in the downstream direction. In between those regions (i.e., in region B), the liquid separation rate increased along the downstream direction because of the interaction between the reverse flow (by the flow recirculation in region C) and the forward flow (in region A). For region A, the liquid separation rate could be successfully predicted by Lee [2] by using the model of the same authors (Lee [7] and Lee and Lee [8]) that has been developed to represent the flow split at parallel T-junctions.

Some practical techniques have been implemented in header-channels assembly of two-phase heat exchangers. Those are installations of flow restrictions or guides at the inlet and/or the inside of the header, and separation and remix of the gas and liquid phases (Hrnjak [4]). One of them, channel protrusion to the header is useful technique to achieve uniform flow distribution. Related with the previous studies for that technique, Lee and Lee [3] reported a typical result

\* This paper was recommended for publication in revised form by Associate Editor  
Yang Na

<sup>†</sup> Corresponding author. Tel.: +82 55 249 2613, Fax: +82 55 249 2617  
E-mail address: jklee99@kyungnam.ac.kr

© KSME & Springer 2010

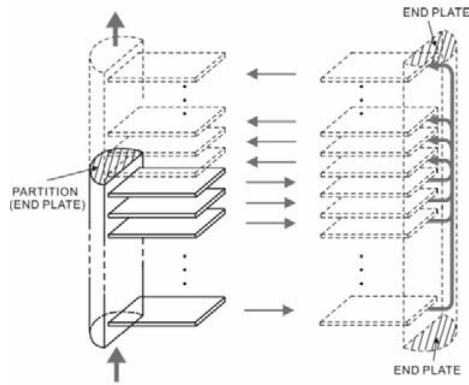


Fig. 1. Illustration of the header-channels flow in a 2-pass heat exchanger.

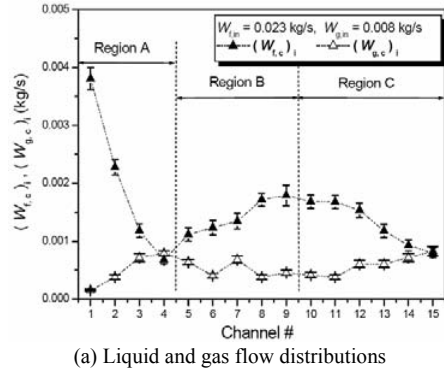


Fig. 2. Typical flow distribution shapes and illustration of flow configuration (Lee [2]).

showing the effect of the intrusion (protrusion) depth on the flow distribution using a test section having six horizontal parallel channels ( $22 \text{ mm} \times 1.8 \text{ mm}$ ) connected to a header ( $24 \text{ mm} \times 24 \text{ mm}$ ). According to them, the optimum intrusion depth for even distribution of the liquid and gas flows to each channel turned out to be 3 mm. Koyama et al. [9] investigated the effect of varying the tube protrusion depth for a horizontal round header (9 mm ID) - six vertical flat tube configuration

Table 1. Experimental conditions.

Inlet Conditions	Ranges	Geometric Variables	Ranges
$G_{in}, \text{kg/m}^2\text{s}$	$70 - 165$	$S, \text{mm}$	$10, 21.6$
$x_{in}$	$0.3 - 0.7$	$H/D_h$	$0 - 0.5$
		$D_h, \text{mm}$	14

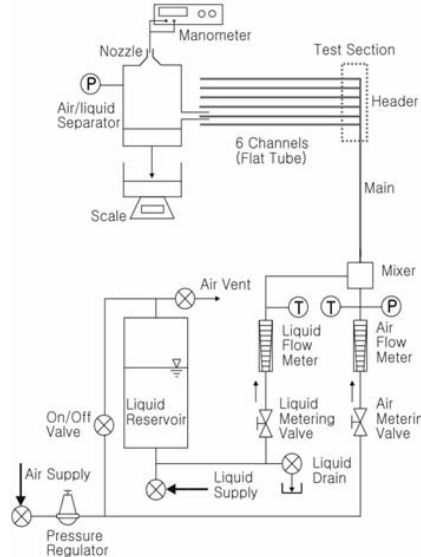


Fig. 3. Experimental setup.

using R-134a. Tests were conducted for the downward configuration, and the flow at the header inlet was identified as intermittent. The protrusion depth was varied, and the optimum configuration was found to be with front two tubes protruded to the center of the header and the remaining four tubes flush-mounted. Better liquid distribution was obtained at a lower vapor quality. Kim et al. [10] also checked the effect of the intrusion depth for various cases. The tube intrusion depth ( $H$ ) has been changed up to  $D/2$ . In the case of downward flow, more water was forced to flow to the rear part of the header with increasing of the protrusion depth as well as increasing of the mass flux and quality. In the case of the upward flow, flow distribution was not much affected by the intrusion depth, mass flux and quality. However, the previous results are only applicable to limited test conditions, and should be generalized by testing various header-channels configuration and a wider range of inlet conditions.

In the present study, as an extension of the previous work, the proper intrusion depths ( $H$ ) for even flow distribution are sought for various header inlet conditions ( $G_{in}, x_{in}$ ) and the spacing between the channels ( $S$ ) that can cover most of the ranges of the flow and geometrical configurations of compact heat exchangers.

## 2. Experimental setup

Fig. 3 illustrates the experimental setup. Air and water were used as the test fluids and the both were measured by using

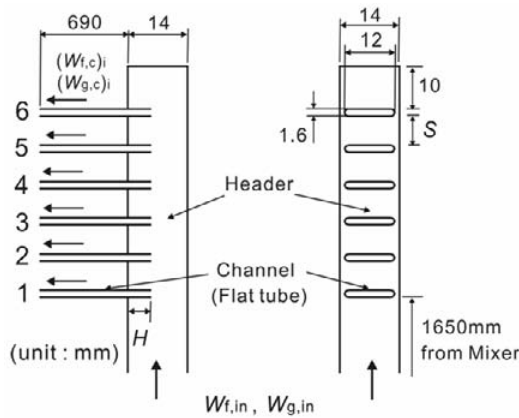


Fig. 4. Configuration of test section.

calibrated rotameters (Dwyer Co.). As shown in Fig. 4, the distance from the mixer to the header inlet was 1650mm. The vertical square header ( $14 \text{ mm} \times 14 \text{ mm}$ ,  $D_{h,\text{in}} = 14 \text{ mm}$ ) was made of transparent acrylic plates for flow visualization. Six (6) rectangular horizontal channels ( $12 \text{ mm} \times 1.6 \text{ mm}$ ), made of aluminum, were connected in parallel to the header. The air/water mixture flowed out through the channels to the air/liquid separator maintained at the atmospheric pressure condition. The flow rate of air was estimated from the velocity measured at the outlet of the converging nozzle (30 mm in diameter) of the separator, using a pitot tube along with a manometer (FCO12, Furness Co.). The water flow rate was measured by weighing the mass of the water collected at the bottom of the separator for a given period of time.

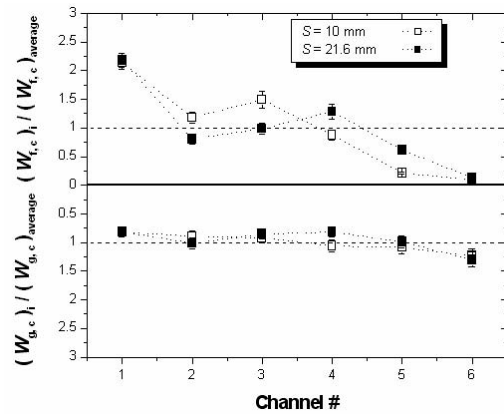
The experiments were carried out for the annular flow regime at the header inlet. This is because the annular flow pattern is mostly probable to occur once the mass quality becomes large (say, larger than 0.1). The flow pattern was also confirmed with the flow regime map of Troniewski and Ulbrich [11] that had been constructed to identify the flow patterns in a vertical rectangular channel with the hydraulic diameter range of 7.4-13.3 mm. Inlet mass flux and quality ranges of air/water mixture are shown in Table 1. Also, the distance ( $S$ ) between the channels and the intrusion depth ( $H$ ) tested are given in the same table. Since the exit of the parallel channels was kept at the atmospheric pressure condition, the pressure within the header inlet should be higher by 50 to 100 kPa depending on the operating condition.

Measurements were repeated for three times for each experimental condition. The measurement uncertainties for the liquid and gas flow rates through the channels stayed within  $\pm 9\%$  and  $\pm 7\%$ , respectively, depending on the flow rates and indicated as error bars in the corresponding plots afterwards.

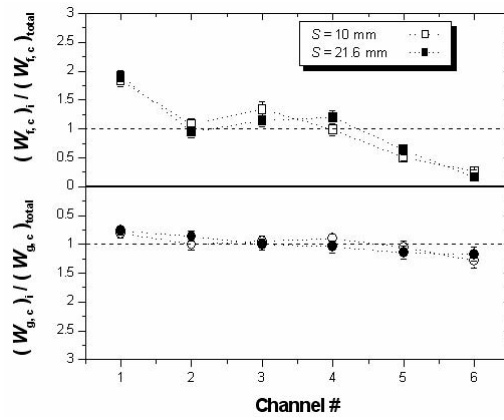
### 3. Experimental results

#### 3.1 Effect of channel (branch) spacing ( $S$ )

Fig. 5 shows the distribution patterns of the liquid and gas flows to the channels for different channel distances and flow



(a)  $G_{\text{in}} = 100 \text{ kg/m}^2\text{s}, x_{\text{in}} = 0.7$



(b)  $G_{\text{in}} = 100 \text{ kg/m}^2\text{s}, x_{\text{in}} = 0.5$

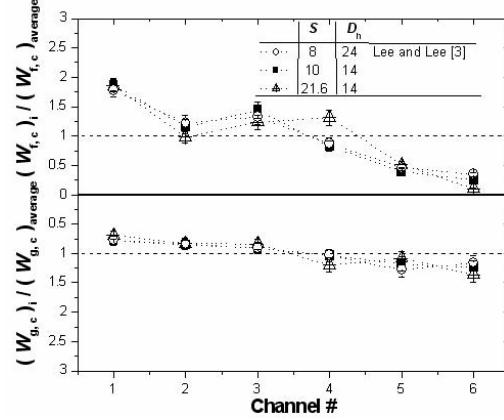
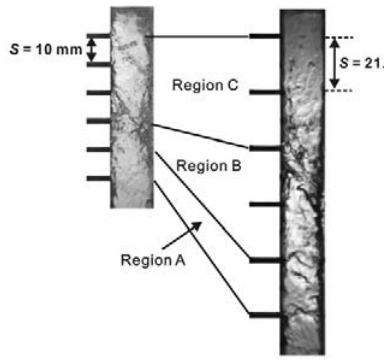


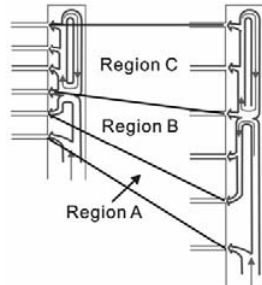
Fig. 5. Effect of distance between channels ( $S$ ) ( $H = 0$ ).

rates and qualities of the two-phase mixtures at the header inlet, but with the zero intrusion depth. Basically, the distribution patterns are the same with that shown in Fig. 2, tested with 15 channels by the same author (Lee [2]); that is, the rate of the liquid separation decreases and then increases, and decreases again along the downstream direction of the header. The only different thing is the relative size of each region. With the larger channel distance, the relative size of region C becomes smaller while that of region A remains unchanged.



$G_{in} = 70 \text{ kg/m}^2\text{s}$ ,  $x_{in} = 0.45$

(a) Flow visualization



(b) Schematic flow configuration

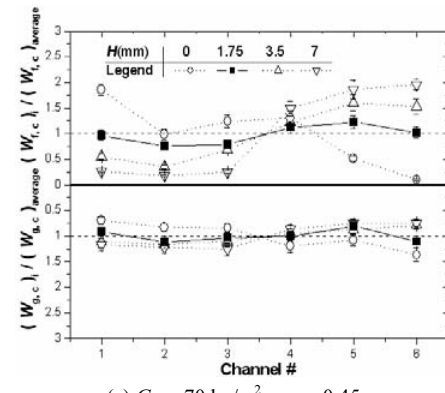
Fig. 6. Effect of distance between channels ( $S$ ) on flow configuration inside header.

Thus region B appears to be larger. To help understanding the trend of the flow distribution, the flow visualization result using CCD camera (Phantom, Vision Research) with 2000 frames/sec is shown in Fig. 6(a), and shows an illustration of the channel spacing effect on the header flow configuration in Fig. 6(b).

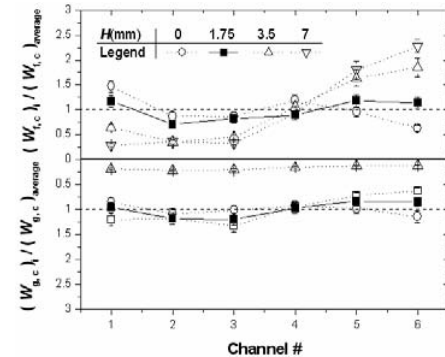
In Fig. 5(c), the results by Lee and Lee [3] were plotted together for comparison. Again, the trend is the same even though the sizes of the header and the channel cross-sections are different. It should be mentioned that the header cross-section size ranging between 14 and 24 mm appears less influential than the channel distance. The gas flow distribution pattern is almost insensitive to the channel distance and the header size.

### 3.2 Effect of intrusion depth

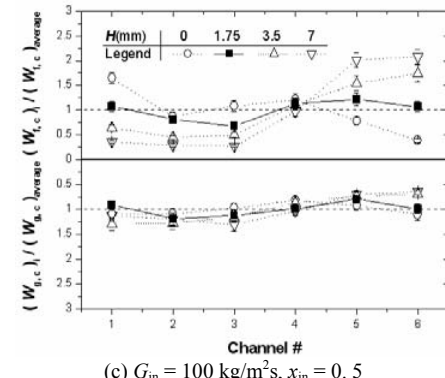
Fig. 7 shows the effect of the channel intrusion depth on the flow distributions for two different flow rates and qualities at the header inlet conditions. Regardless of the header inlet conditions, dependence of the flow distribution patterns on the intrusion depth appeared to be the same. In other words, for zero intrusion depth ( $H = 0$ ), though there is a local increasing region (denoted as region B in Fig. 2), more amount of liquid is split out to the channels at the fore part of the header. On the other hand, the trend becomes reversed with a deep intrusion depth ( $H = 7 \text{ mm}$ ). This is because the intruded part hinders the liquid flow (liquid film) inside the header from being separated out through the channels (This can be confirmed through flow



(a)  $G_{in} = 70 \text{ kg/m}^2\text{s}$ ,  $x_{in} = 0.45$



(b)  $G_{in} = 120 \text{ kg/m}^2\text{s}$ ,  $x_{in} = 0.35$



(c)  $G_{in} = 100 \text{ kg/m}^2\text{s}$ ,  $x_{in} = 0.5$

Fig. 7. Effect of intrusion depth ( $H$ ) on flow distribution. ( $D_h = 14 \text{ mm}$ ,  $S = 21.6 \text{ mm}$ ).

visualization as demonstrated in Fig. 8(a) for  $H/D_h = 1/2$ ). The same trend has been reported by Lee and Lee [3]. Therefore, though the spacing between the channels ( $S$ ) is increased from 8 mm to 21.6 mm, the effect of the intrusion depth on the flow distribution is very large. This tells that there should be an optimum value of the intrusion depth for even flow distribution, staying between zero and 7 mm; and the test results give 1.75 mm as the optimum value (Figs. 7(a), (b) and (c)), corresponding to 1/8 of the header hydraulic diameter. The same results were obtained for  $H/D_h = 1/8$  with different channel spacing as shown in Fig. 9. The results of Lee and Lee [3] ( $S = 8 \text{ mm}$ ) were also plotted to show the same value of the optimum intrusion depth,  $D_h/8$ .

The flow behavior with the optimum value of  $H/D_h$  is visu-

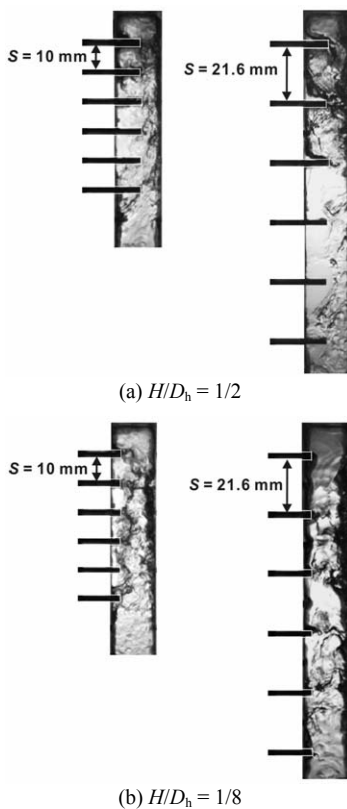


Fig. 8. Flow visualization of effect of intrusion depth ( $H$ ) on flow configuration with different distance between channels ( $D_h = 14$  mm,  $G_{in} = 70$  kg/m<sup>2</sup>s,  $x_{in} = 0.45$ ).

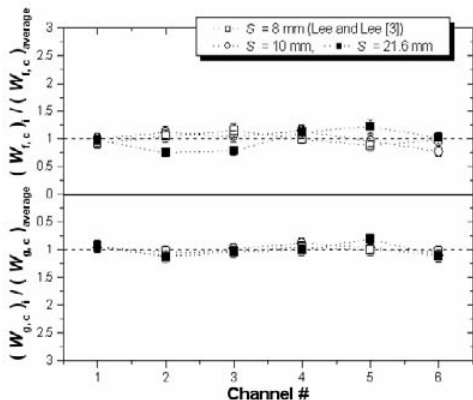


Fig. 9. Effect of distance between channels with different intrusion depths ( $H/D_h = 1/8$ ,  $G_{in} = 70$  kg/m<sup>2</sup>s,  $x_{in} = 0.45$ ).

alized in Fig. 8(b). The photographs show that the liquid and the gas flows inside the headers are well mixed with each other regardless of the distance between the channels. As a consequence, the liquid flow distribution to the channels tends to be even. It can be tentatively concluded that the ratio of the optimum intrusion depth to the header size ( $H/D_h$ ) appears to be about the same, 1/8, for practical ranges of the flow rate ( $G_{in}=70\text{-}165$  kg/m<sup>2</sup>s), mass quality ( $x_{in}=0.3\text{-}0.7$ ), channel distance ( $S=8\text{-}21.5$  mm) and the header size ( $D_{h,in}=14\text{-}24$  mm). At the same time, the gas separation rate to the channels re-

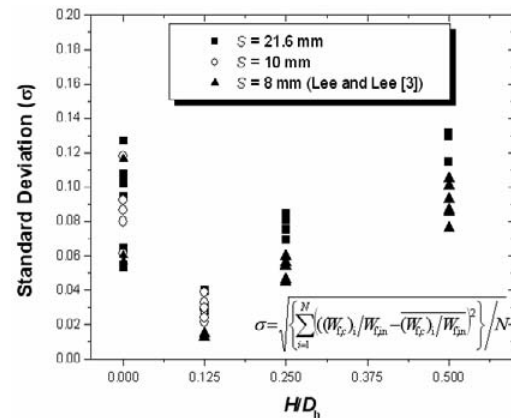


Fig. 10. Standard deviation of liquid flow distribution with intrusion depth ( $H$ ).

mains even as shown in Fig. 9.

The standard deviations from the mean values of the liquid separation rates through the channels for each test condition were given as Fig. 10. As clearly seen in this figure, at  $H/D_h=1/8$ , the absolute value of the standard deviation becomes a minimum, which corresponds with the optimum intrusion depth.

#### 4. Conclusion

The pattern of the liquid distribution from the header to the parallel channels is relatively insensitive to the channel spacing, and the effect of the header cross-section size ( $D_{h,in}=14\text{-}21$  mm) appears to be even minor. On the other hand, the intrusion depth of the channels to the header wall changes the distribution pattern seriously. Throughout a series of the experiments, the optimum intrusion depth was identified to be 1/8 of the header hydraulic diameter for the experimental ranges covered in the present work.

#### Acknowledgements

This work was supported by Kyungnam University Foundation Grant, 2010.

#### Nomenclature

$A$	: Area [m <sup>2</sup> ]
$D$	: Diameter [m]
$D_h$	: Hydraulic diameter [m]
$G$	: Mass flux [kg/m <sup>2</sup> s]
$H$	: Intrusion depth [m]
$S$	: Distance between the channels (branches) [m]
$W$	: Mass flow rate [kg/s]
$x$	: Quality [-]

#### Subscripts

c	: Channel
f	: Liquid

g : Gas  
 i : Index (channel numbers)  
 in : Header (main tube) inlet

## References

- [1] T. Kulkarni, C. W. Bullard and K. Cho, Header Design Tradeoffs in Microchannel Evaporators, *Applied Thermal Engineering*, 24 (2004) 759-776.
- [2] J. K. Lee, Two-phase flow behavior inside a header connected to multiple parallel channels, *Experimental Thermal and Fluid Science*, 33 (2009) 195-202.
- [3] J. K. Lee and S. Y. Lee, Distribution of two-phase annular flow at header-channel junctions, *Experimental Thermal and Fluid Science*, 28 (2004) 217-222.
- [4] P. Hrnjak, Developing Adiabatic Two Phase Flow in Headers - Distribution Issue in Parallel Flow Microchannel Heat Exchangers, *Heat Transfer Engineering*, 25 (2004) 61-68.
- [5] P. Fei, Dj. Cantrak and P. Hrnjak, Refrigerant Distribution in the Inlet Header of Plate Evaporators, *SAE Paper 2002-01-0948* (2002) 1397-1402.
- [6] D. Zietlow, M. Campagna and J. Dias, Innovative Experimental Apparatus to Measure Liquid Flow Distribution in Two-phase Flow Occurring in the Manifolds of Compact Heat Exchangers, *ASHRAE Trans.*, 108 (2002).
- [7] J. K. Lee, Branching of two-phase flow from a vertical header to horizontal parallel channels, *Journal of Mechanical Science and Technology*, 23 (2009) 1628-1636.
- [8] J. K. Lee and S. Y. Lee., Assessment of prediction models for dividing two-phase flow at small T-junctions, *Int. J Heat exchangers*, 6 (2005) 217-234.
- [9] S. Koyama, A. T. Wijayanta, K. Kuwahara and S. Ikuda, Developing Two-Phase Flow Distribution in Horizontal Headers with Downward Micro-Channel Branches, *Proceedings of the 11th Int. Refrigeration and Air Conditioning Conference at Purdue*, (2006) R142.
- [10] N. H. Kim and T. R. Shin, Two-phase flow distribution of air-water annular flow in a parallel flow heat exchanger, *Int. J. Multiphase Flow*, 32 (2006) 1340-1353.
- [11] L. Troniewski and R. Ulbrich, Two phase gas liquid flow in rectangular channels, *Chem. Eng. Sci.*, 39 (1984) 751-765.



**Jun Kyung Lee** received his B.S. degree in Mechanical Engineering from Busan National University in 1999. He then received his M.S. and Ph.D. degrees from KAIST in 2001 and 2005, respectively. Dr. Lee is currently a Professor at the School of Mechanical Engineering and Automation at Kyungnam University in Masan, Korea. Dr. Lee's research interests are in the area of two-phase flow and heat transfer, micro-fluidics, cryogenic devices for superconductivity, thermal management system for automobile.